Figure S1

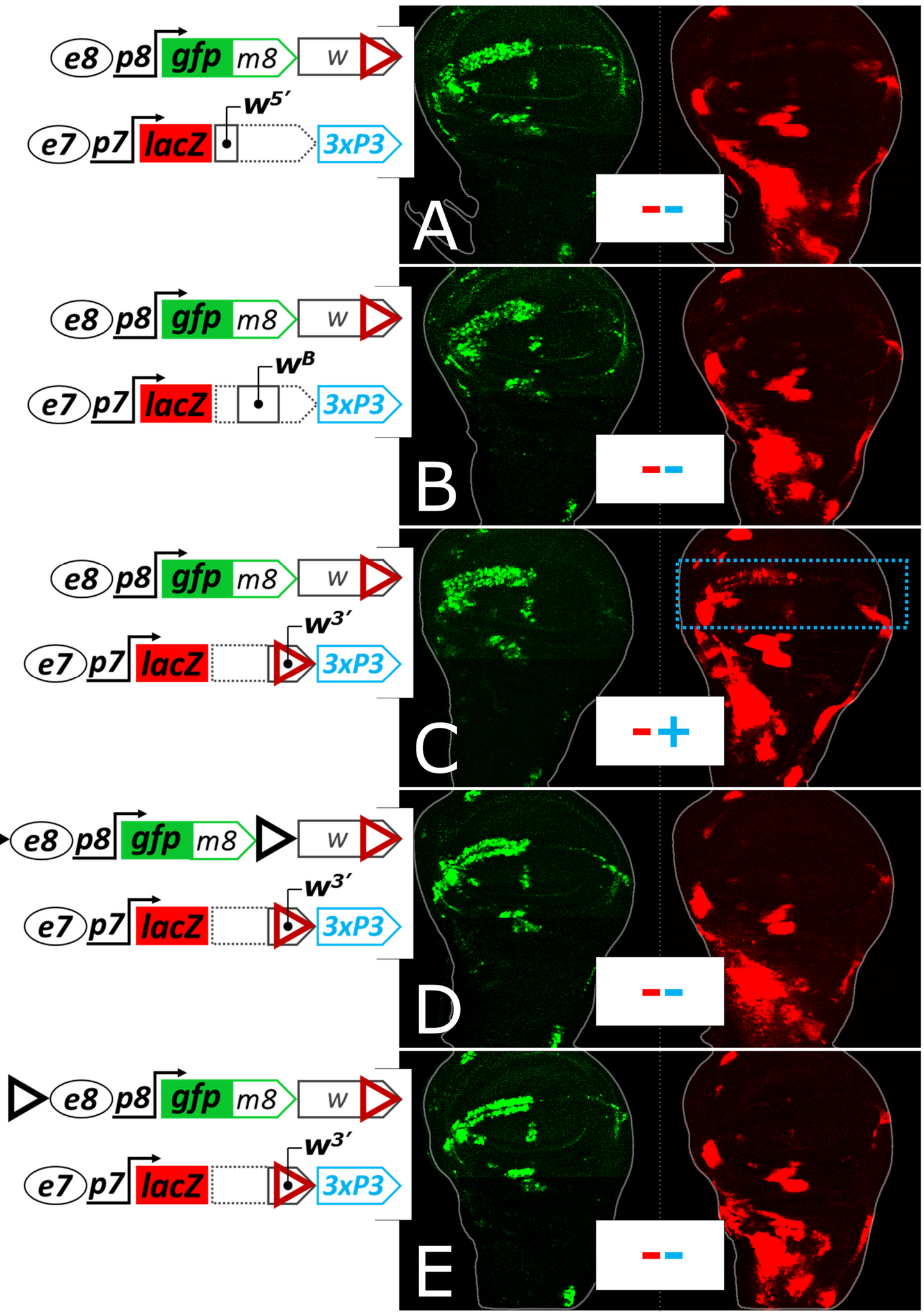

Figure S1 *White*-mediated uni-directional transvection relies on the mini-*white*-contained Wari insulator (WI). Three fragments of mini-*white*, cloned in the *e7p7-lacZ-3xP3* construct, were tested in the *attP40* locus in a transvection assay against an *e8p8-EGFPm8* transgene containing full-sized mini-*white* (**A**-**C**). Neither promoter region of mini-*white* ($w^{5'}$, 0.24 kb, **A**), nor its 'gene body' (w^{B}, 2.4 kb, **B**) mediated transvection; whereas the 3' part of mini-*white* ($w^{3'}$, 0.9 kb, **C**) did exhibit uni-directional transvection in WM (blue dotted rectangle; blue + sign). This fragment is known to contain WI. Addition of one or two GIs in the *e8p8* construct inhibited WI-mediated transvection (**D**-**E**). + and – signs refer to presence and absence of transvection, respectively; red refers to *e7→p8* transvection (GFP in AMPs) and blue refers to *e8→p7* transvection (LacZ in the WM).

Figure S2

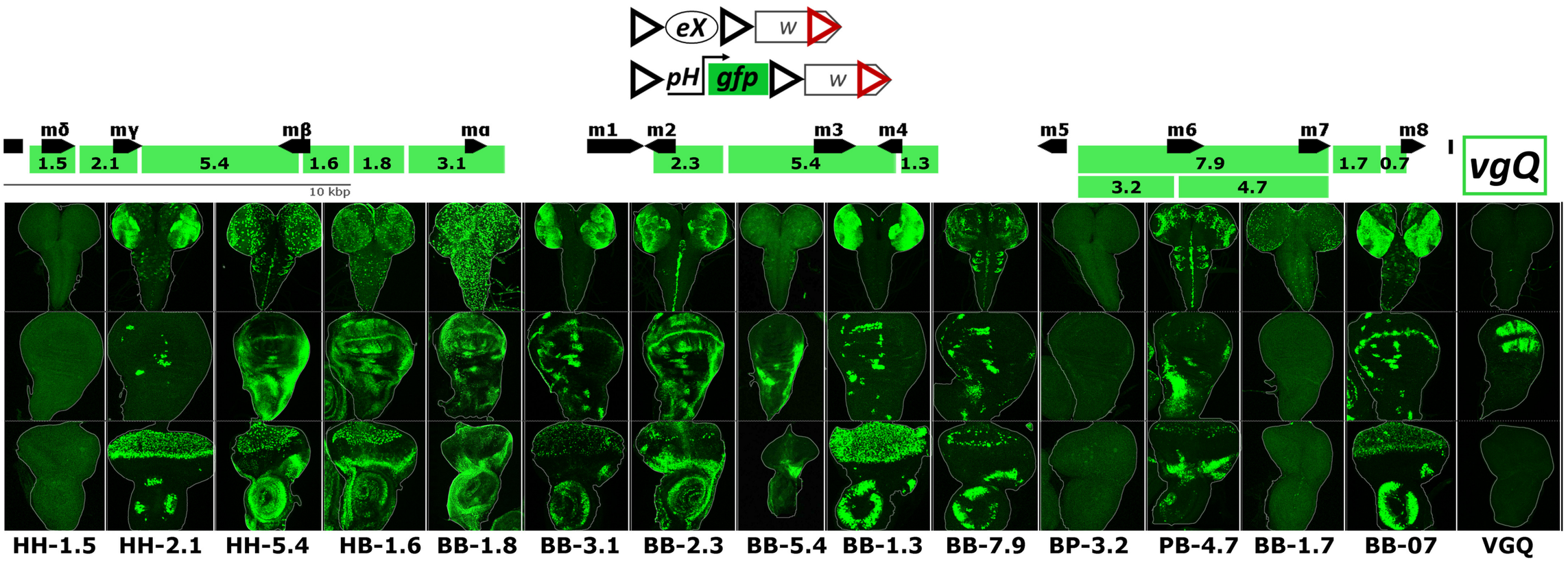

Figure S2 GI-mediated transvection is compatible with many developmental enhancers. A map of the *E(spl)* locus is shown on top and DNA fragments are marked as green rectangles with indicated length in kb. Each of these DNA fragments ('*eX*' in the constructs' scheme) was inserted into a transgene between GIs, placed in *trans* to GIs-flanked *pH-gfp* transgene in *attP40*. Heterozygotes were tested for activating *pH-gfp* expression in larval CNS (top), wing disk (middle) and eye-antennal disk (bottom row). Another fragment, unrelated to the *E(spl)* locus, the *vestigial* quadrant enhancer (*vgQ,* last column) recapitulates its *cis* activity in *trans* (GFP expression only in the wing disk).

Figure S3

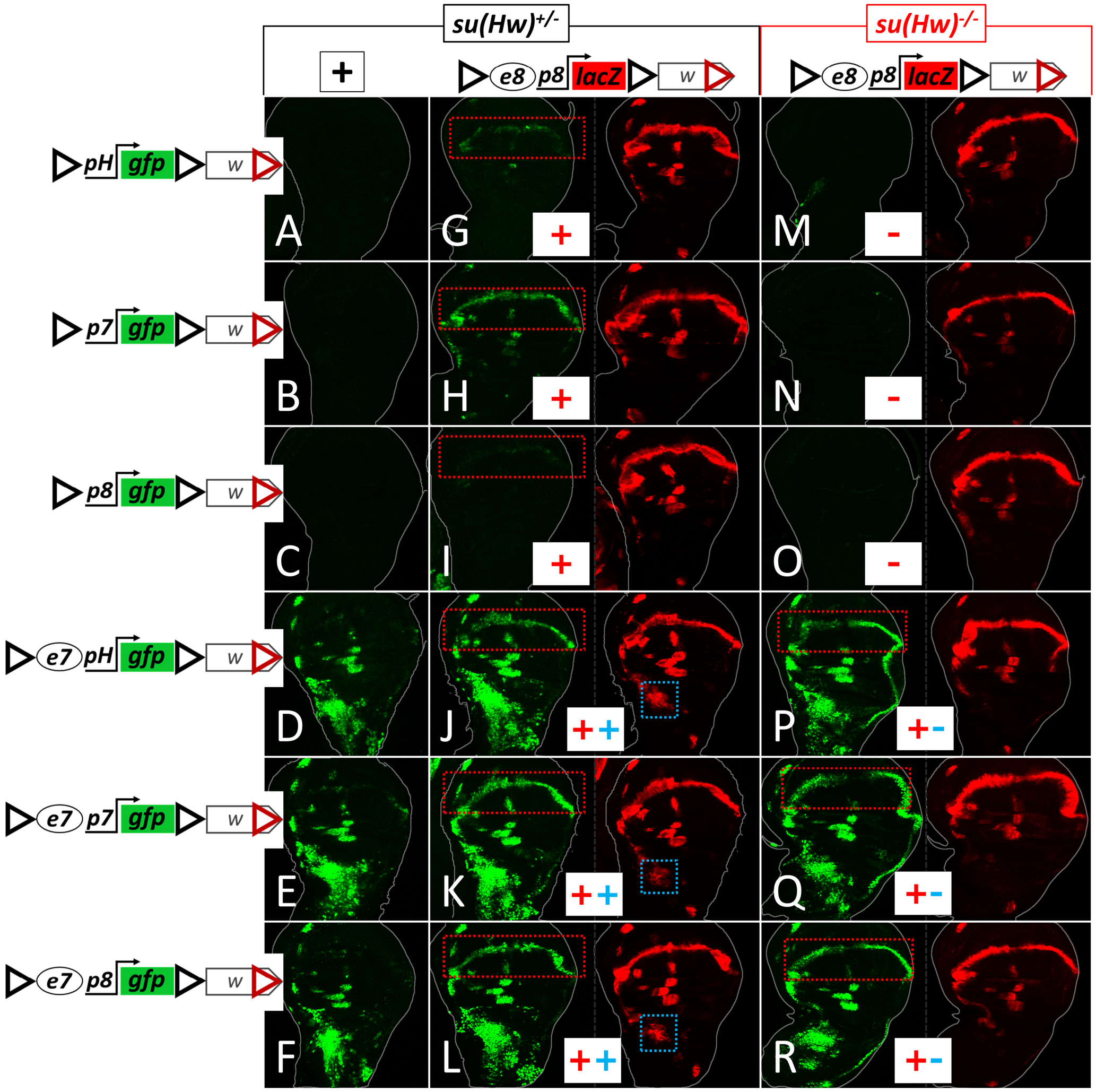

Figure S3 WI-mediated *trans*-activation by the *e8* enhancer requires the presence of the *e7* enhancer on the other homolog. All transgenes contain GIs and mini-*white* and are inserted in *attP40*. (**A**-**F**) Wing disks from animals hemizygous for the indicated GFP transgenes. When GFP is driven by the *pH* promoter (**A**), *E(spl)m7* (*p7*) promoter (**B**) or *E(spl)m8* (*p8*) promoter (**C**), no expression is observed; addition of the *e7* enhancer to any of these promoters (**D**-**F**) results in *e7*-specific expression pattern of the GFP; note the lack of WM expression. **G**-**L** show wing disks from animals heterozygous for the same *gfp* **A**-**F** transgenes and *e8p8-lacZ.* **M**-**R** show the same transgene combinations in disks derived from *su(Hw)*$^{-/-}$ mutants. Blue and red dotted rectangles highlight cells exhibiting *trans*-activity of *e7* (in AMPs) and *e8* (in WM), respectively. These are also summarized by blue and red signs, respectively. + indicates transvection, - no transvection.

Figure S4

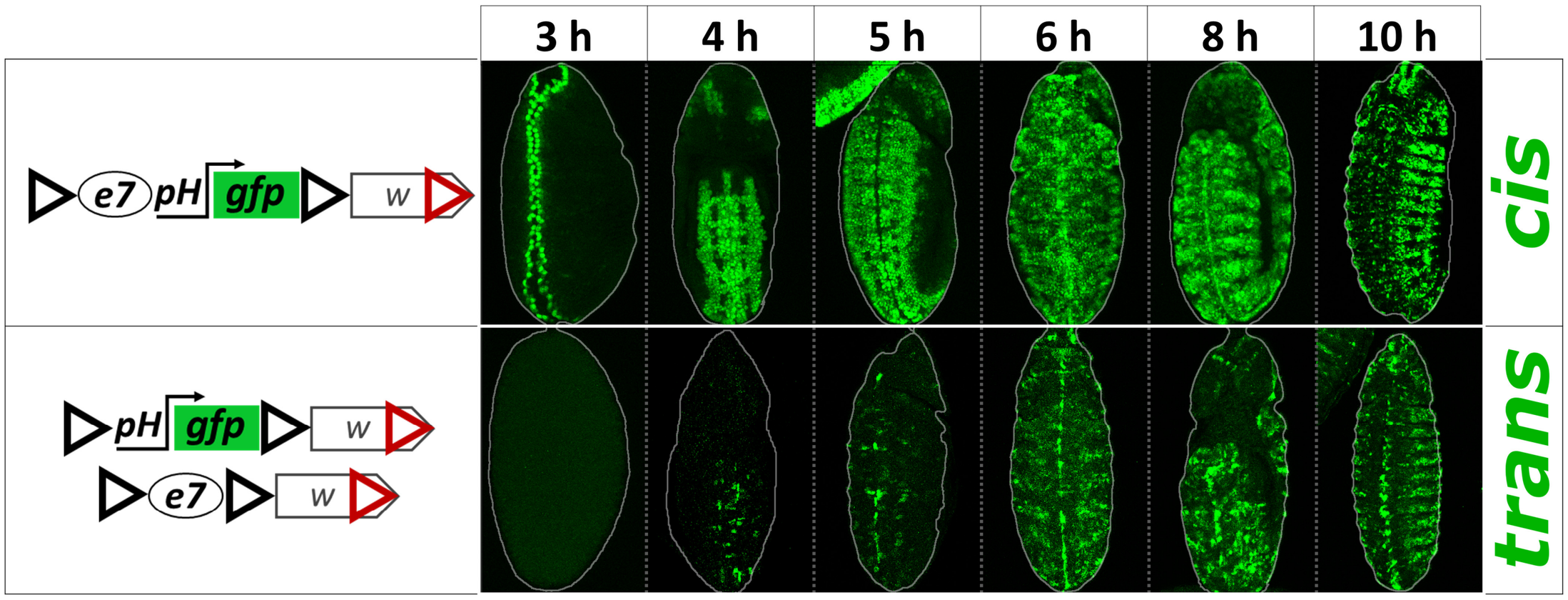

Figure S4 The onset of transvection is delayed in embryogenesis. All embryos are imaged ventrally with anterior to top. A *cis*-linked *e7pH* enhancer-promoter pair (top row) drives GFP expression along the ventral midline within 3 h after egg deposition (AED). At 4-5 h AED *e7pH* is broadly active in the ventral ectoderm, whereas *e7* and *pH* separated in *trans* show interaction only in a small subset of these cells. From 7h AED onwards *e7* and *trans-pH* seem to interact in most cells where *e7*(*cis*-)*pH* is active. The enhancerless *ph-gfp* reporter shows no background expression in embryos as a hemizygote (data not shown). All transgenes are inserted in *attP40.*

Figure S5

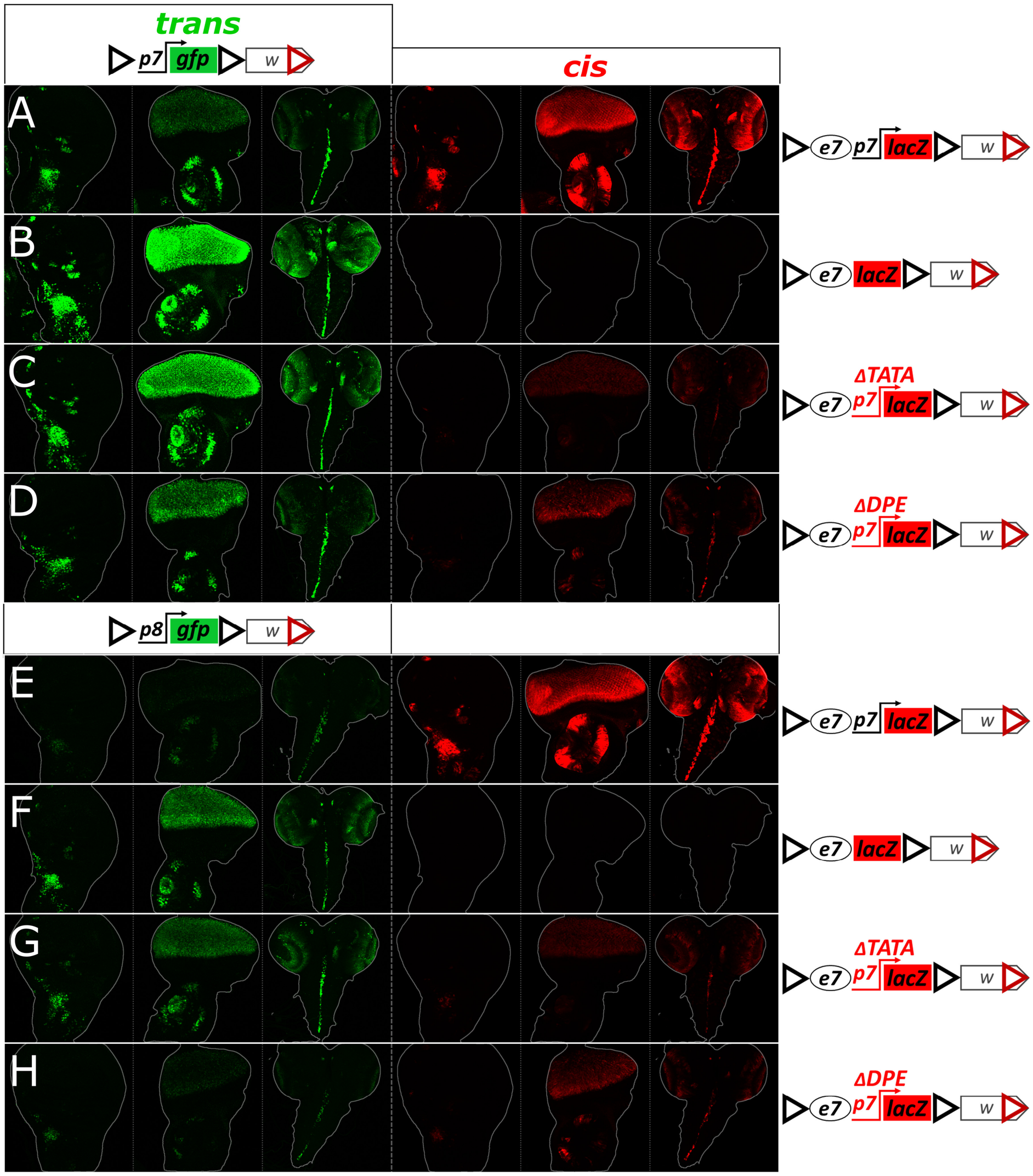

Figure S5 The effects of mutations in the *p7* promoter on the ability of a *cis*-linked *e7* to transvect are independent of the identity of the *trans* promoter. The *e7p7-lacZ* (**A** and **E**) and its derivatives harboring deletions of *p7* (**B** and **F**), *ΔTATA* (**C** and **G**) and *ΔDPE* (**D** and **H**) are placed in *trans* to *p7-gfp* (**A** - **D**) or *p8-gpf* enhancerless reporters (**E** - **H**). For each genotype (each row) the third instar wing disk, eye disk and CNS are examined for *(1)* GFP, reflecting *trans* activity of *e7* on *pH-gfp* (green) and *(2)* β-galactosidase, reflecting *cis* activity the *e7*-linked promoter (red). Although, *p7*, *p8* and *pH* are promoters of different strength, their activity seems to be affected similarly by different mutations in *e7*-linked *p7* (compare to the results obtained for *pH*, **Figure 5**, **D**-**G**). All transgenes contain GIs and mini-*white* and are inserted in *attP40*.

Figure S6

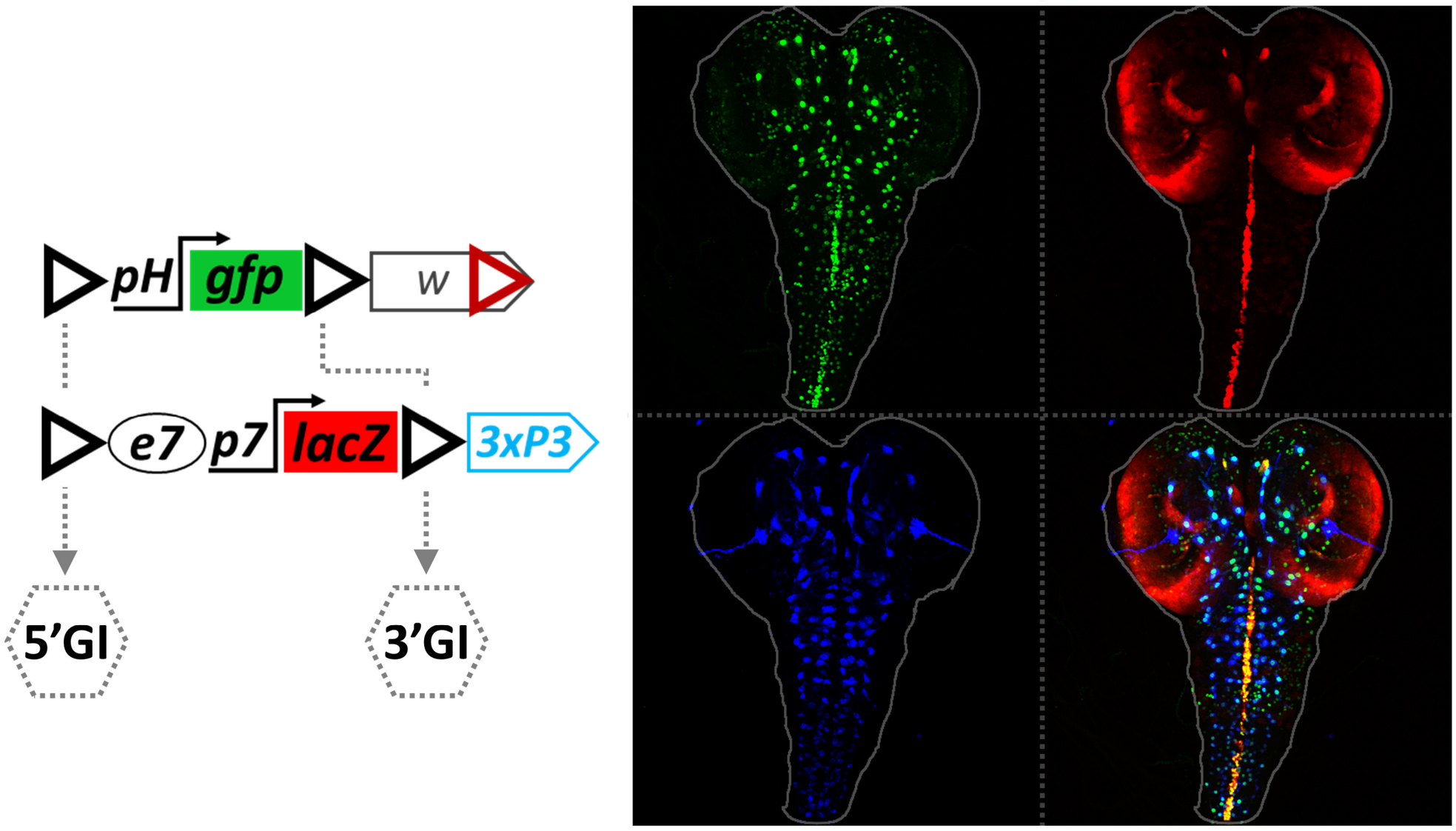

Figure S6 *pH* receives input from two enhancers in *trans*, *e7* and *3xP3*. Confocal z-projection of a third instar CNS from a heterozygote between *e7p7-lacZ-3xP3* and *pH-gfp* dual-GIs^{FOR} transgenes in *attP40*. Top left panel shows *trans*-activated *pH-gfp* expression; note *e7*-specific GFP expression in the VNC midline, corresponding to the *cis*-activity of *e7* (driving expression of LacZ, in red, top right panel), and the 'dotty' *3xP3*-specific expression in central brain and VNC corresponding to glial cells with active *3xP3* enhancer (expressing DsRed, in blue, in *cis,* bottom left panel). Merged image is shown in the bottom right panel.

Figure S7

GI

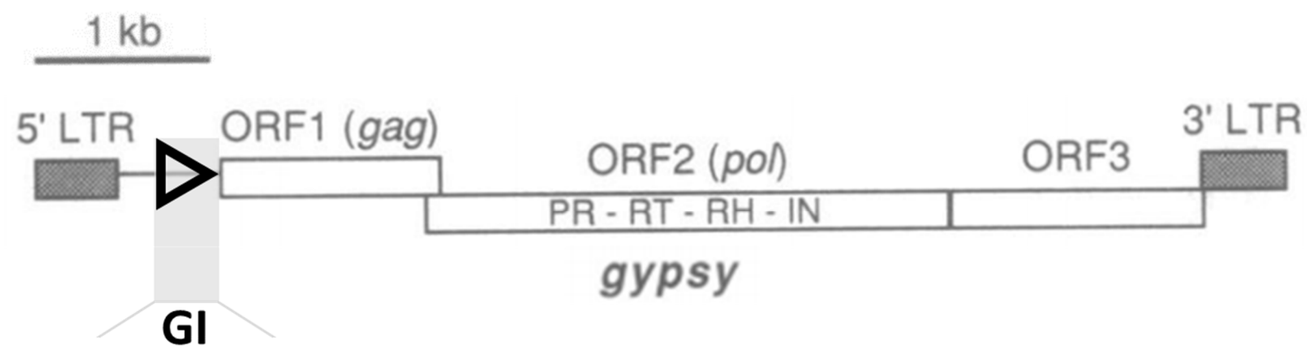

367 bp: 670-1037 (*gypsy retrotransposon*)

WI

368 bp: X:2,788,223..2,792,590 (FlyBase, Dmel r6.26)

Fab8

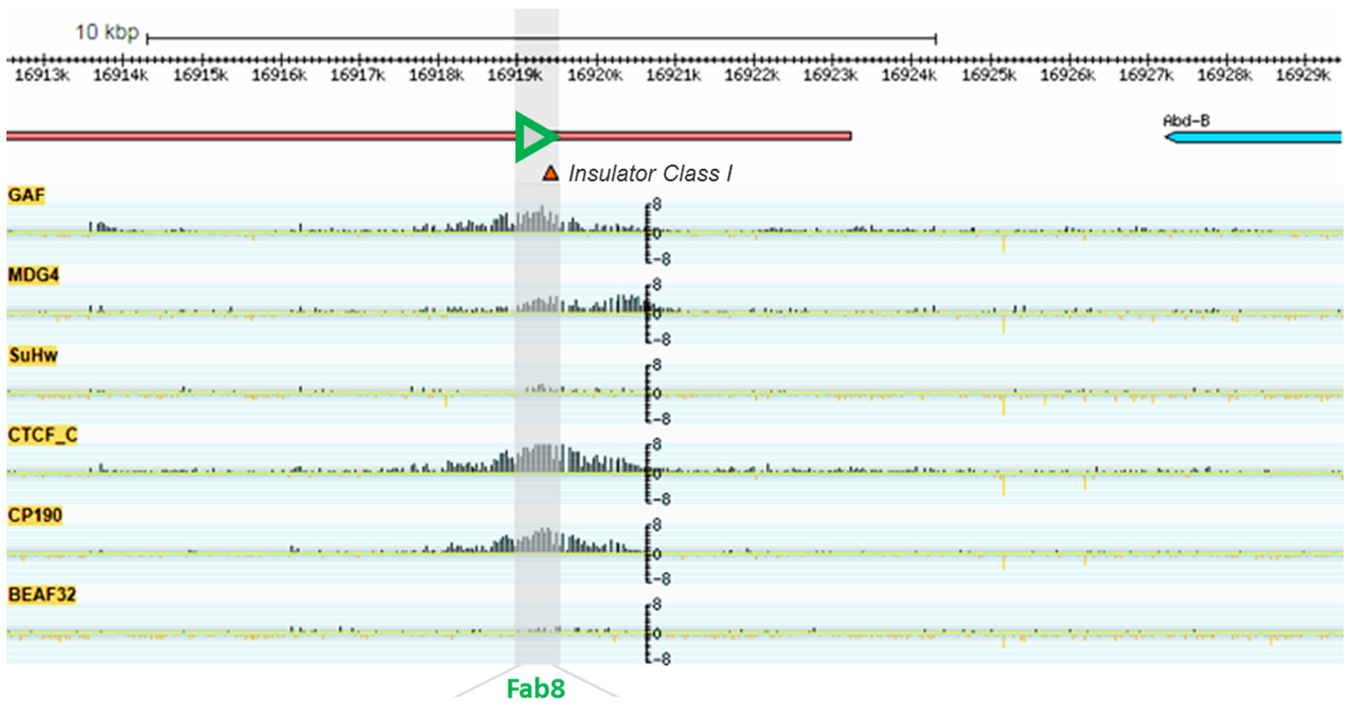

540 bp: 3R:16,918,976..16,919,515 (FlyBase, Dmel r6.26)

1A2

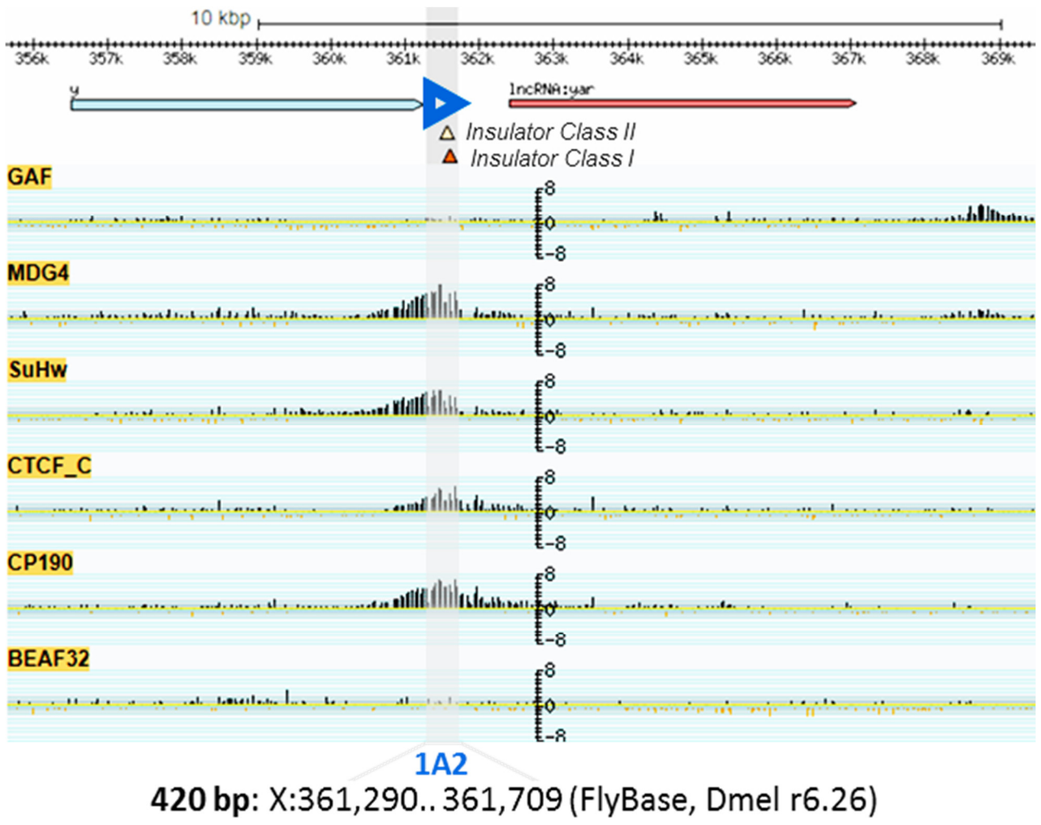

Figure S7 Genomic maps of insulators. Insulators are shown as triangles in the orientation used in the various construct schematics. The position of each insulator is marked in the genome using the genome browser of Flybase (Thurmond *et al.* 2019). Below each genomic map are shown six chromatin-IP tracks for insulator binding proteins derived from modENCODE (Celniker *et al.* 2009) and a peak-calling track for putative insulators (Negre *et al.* 2010), as well as the exact sequence coordinates of the fragment cloned in our constructs. Genomic maps and Ch-IP tracks are not possible for GI, since it comes from a repetitive element; instead the sequence coordinates come from the *gypsy* retrotransposon sequence in Spana *et al.* 1988 and Kim *et al.* 1994.

Figure S8

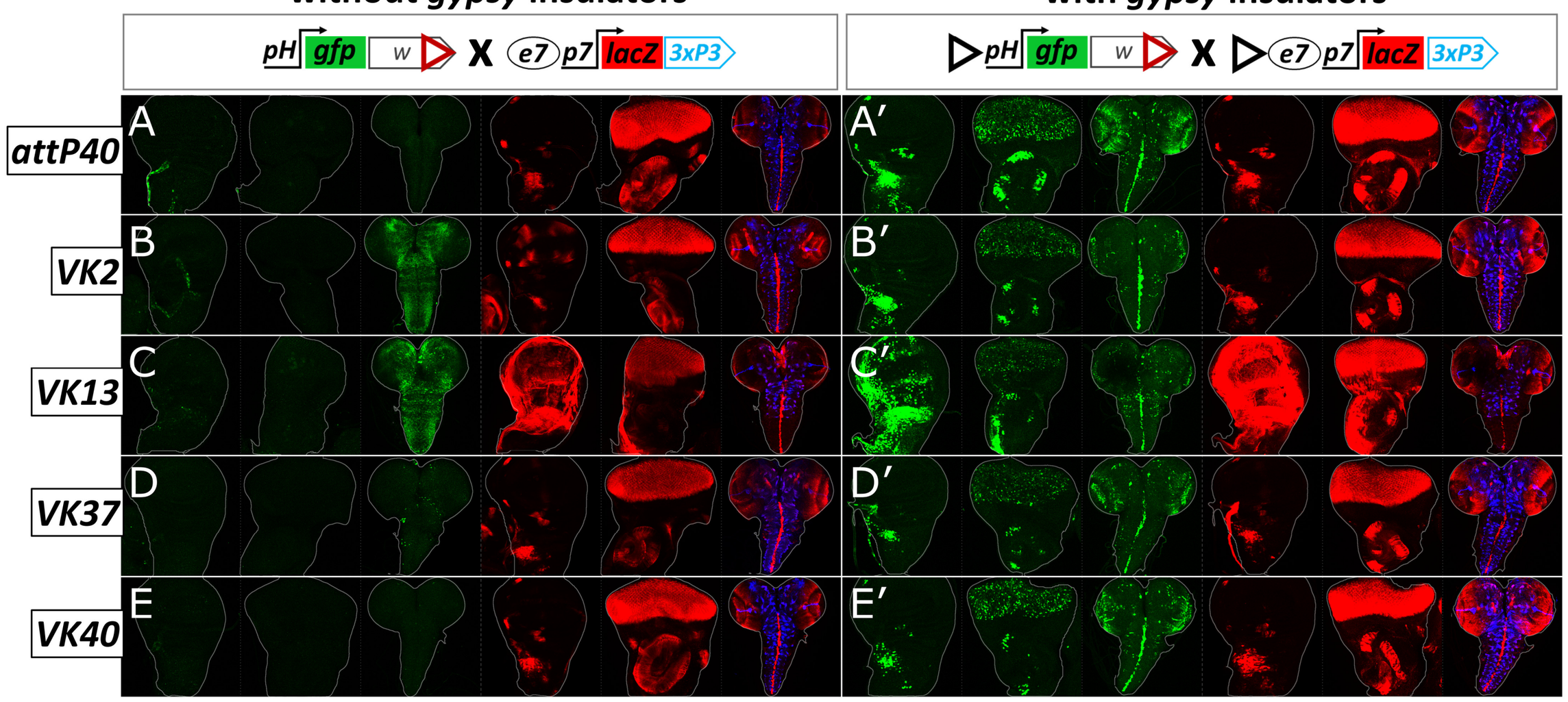

Figure S8 No transvection is observed in the absence of GIs at five different loci. The ability to interact in *trans* was tested between *e7p7-lacZ* and *pH-gfp* transgenes inserted in five genomic loci (*attP40, VK2, VK13, VK37, VK40*) in two configurations of these transgenes: carrying no GIs (**A**-**E**) and containing one 5' GI each (**A'**-**E'**). For each genotype three tissues are shown: wing disk, eye disk and CNS (left to right). Green is *pH*-driven GFP. Red is *e7p7*-driven LacZ. Blue is *3xP3*-driven DsRed (CNS only). Note the activity of neighboring (trapped) enhancers in all loci except *VK40*, which is also seen in the hemizygous condition for these transgenes (not shown): *(1)* tracheal expression in the wing disk of the uninsulated *pH-gfp* in *attP40* and *VK2* and of the GI-insulated *pH-gfp* in *VK37* (**A, B** and **D'**), *(2)* ubiquitous activity in VNC and central brain of the uninsulated *pH-gfp* in *VK2* and *VK13* (**B** and **C**), *(3)* wing pouch activity of the uninsulated *p7-lacZ* in *VK2* (**B**), *(4)* ubiquitous wing disk activity of uninsulated and GI-insulated *p7-lacZ*, and GI-insulated *pH* in *VK13* (**C** and **C'**). Note GFP expression in notum AMPs, eye, antenna, optic lobes and VNC midline in **A'-E'.** All this *e7*-driven GFP expression is absent in **A-E**.

Figure S9

VK2 2L:8,140,863 [-] (FlyBase, Dmel r6.26)

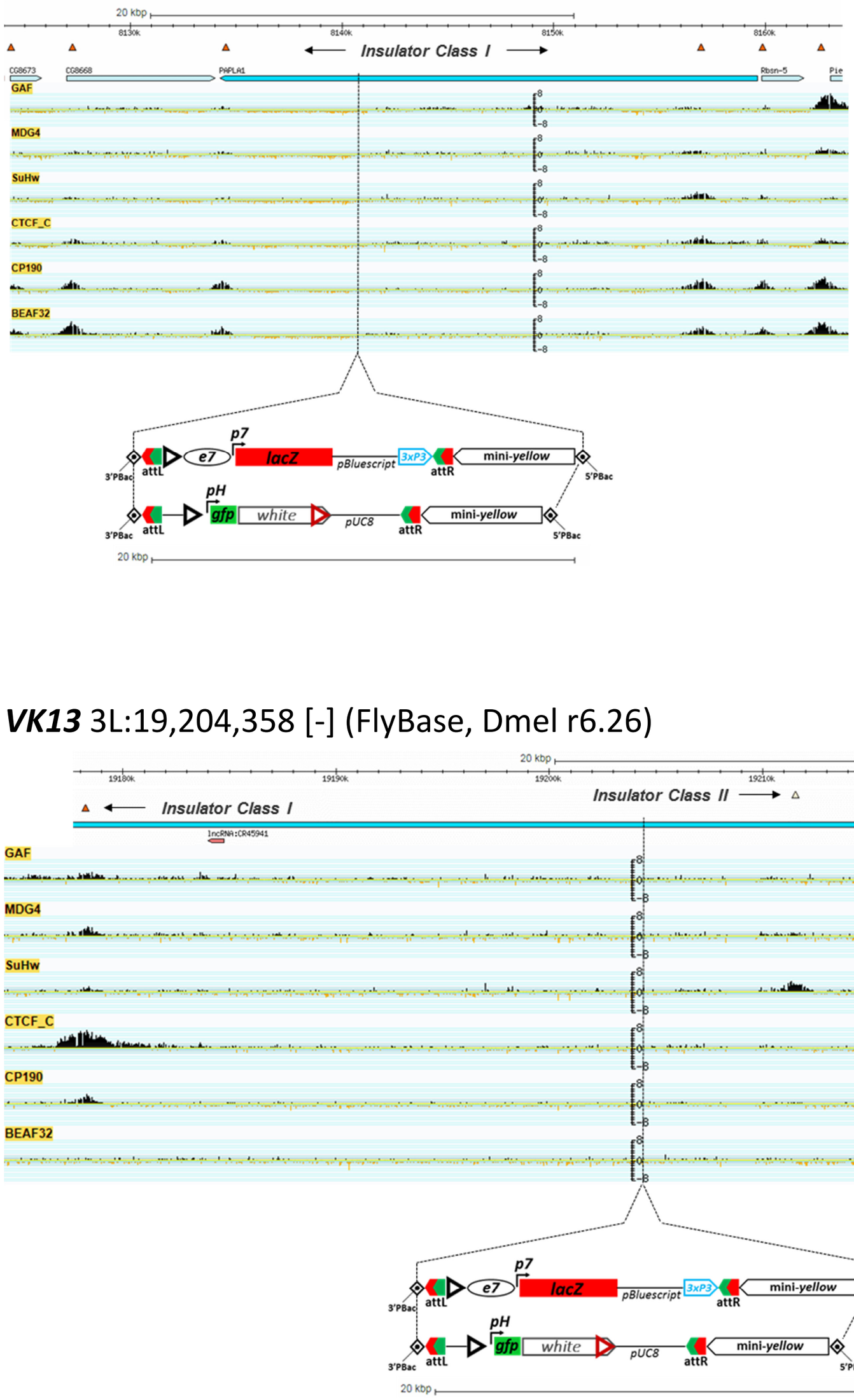

VK13 3L:19,204,358 [-] (FlyBase, Dmel r6.26)

VK37 2L:1,582,820 [+] (FlyBase, Dmel r6.26)

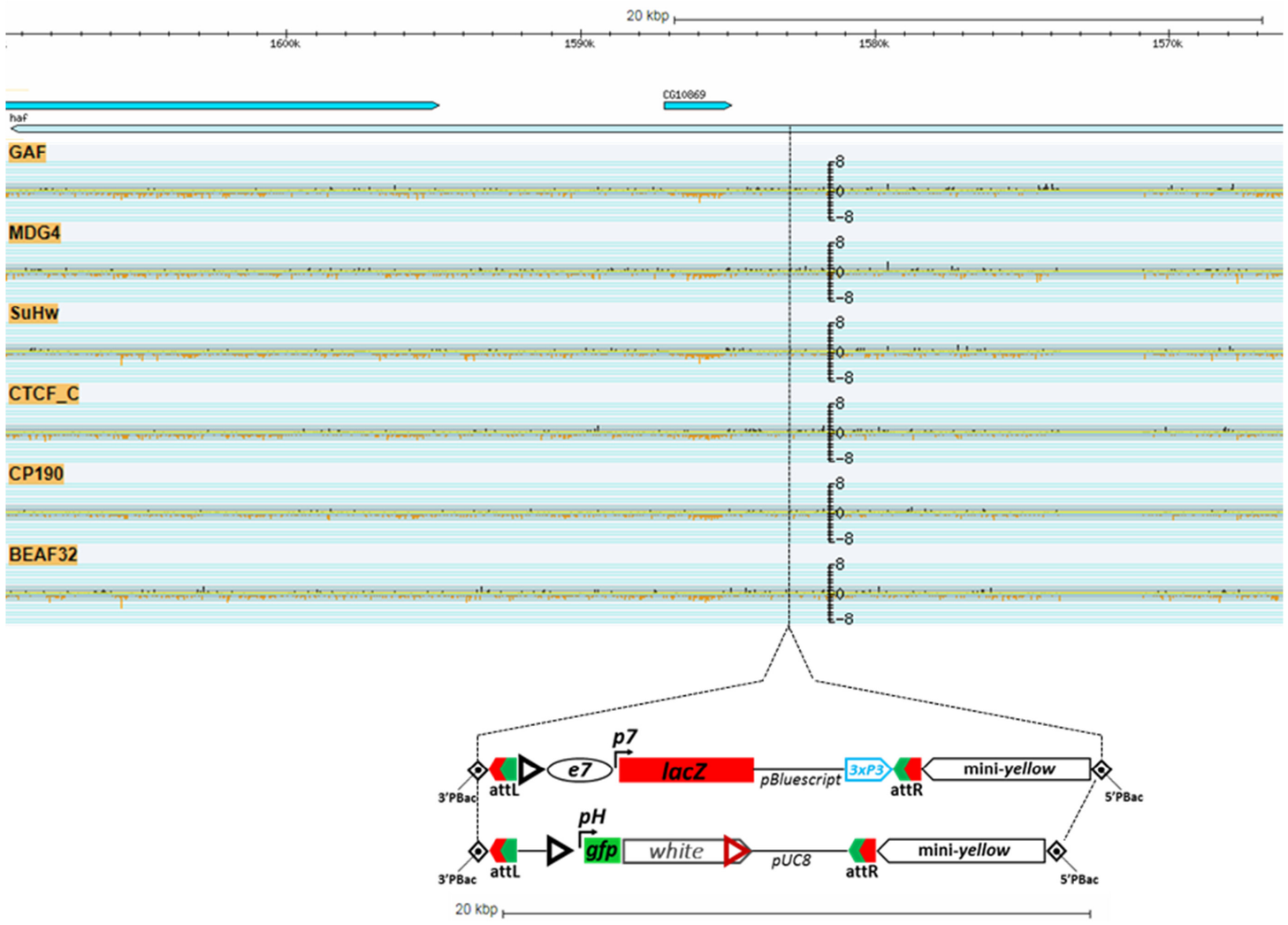

VK40 3R:12,440,193 [-] (FlyBase, Dmel r6.26)

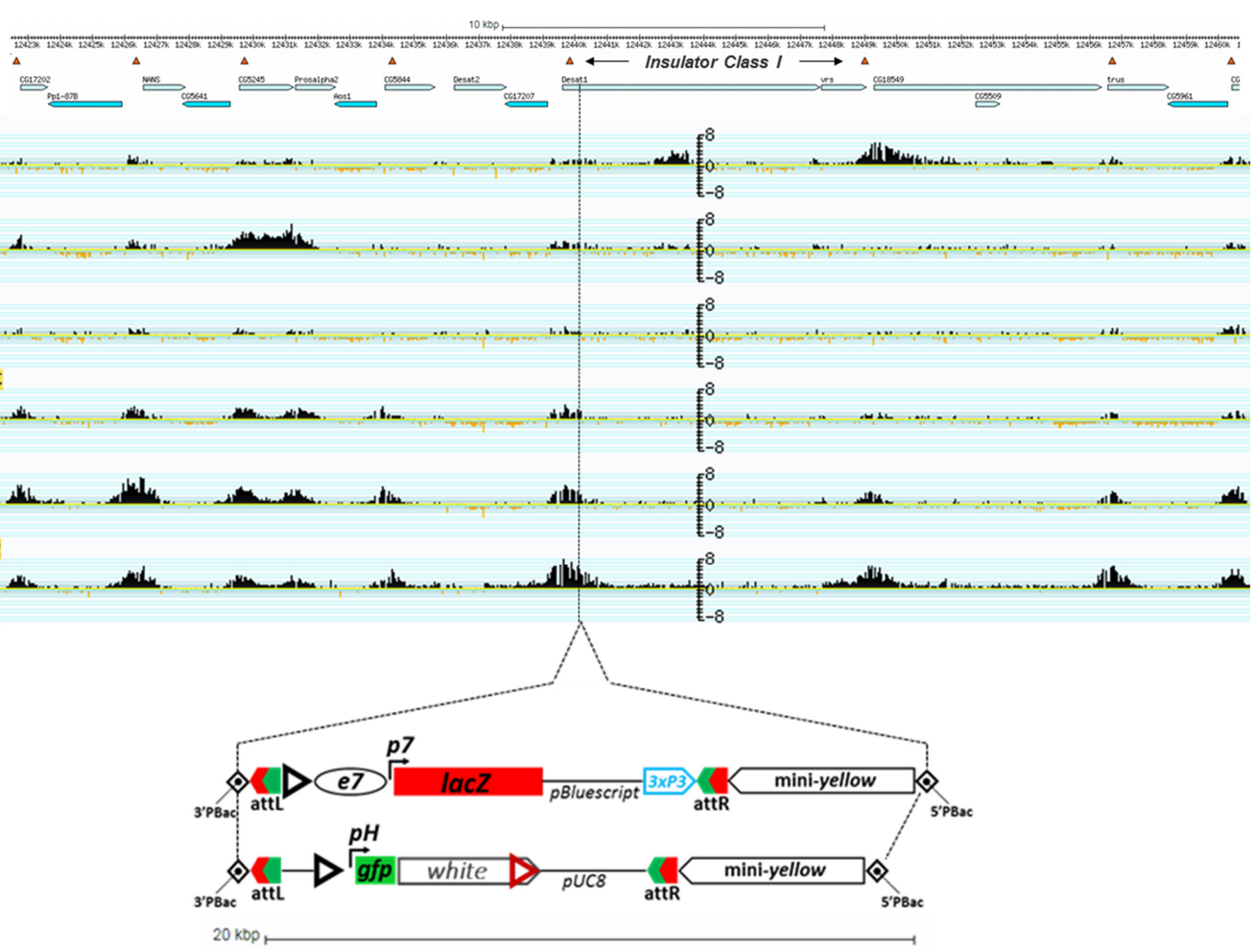

attP40 2L:5,108,448 [-] (FlyBase, Dmel r6.26)

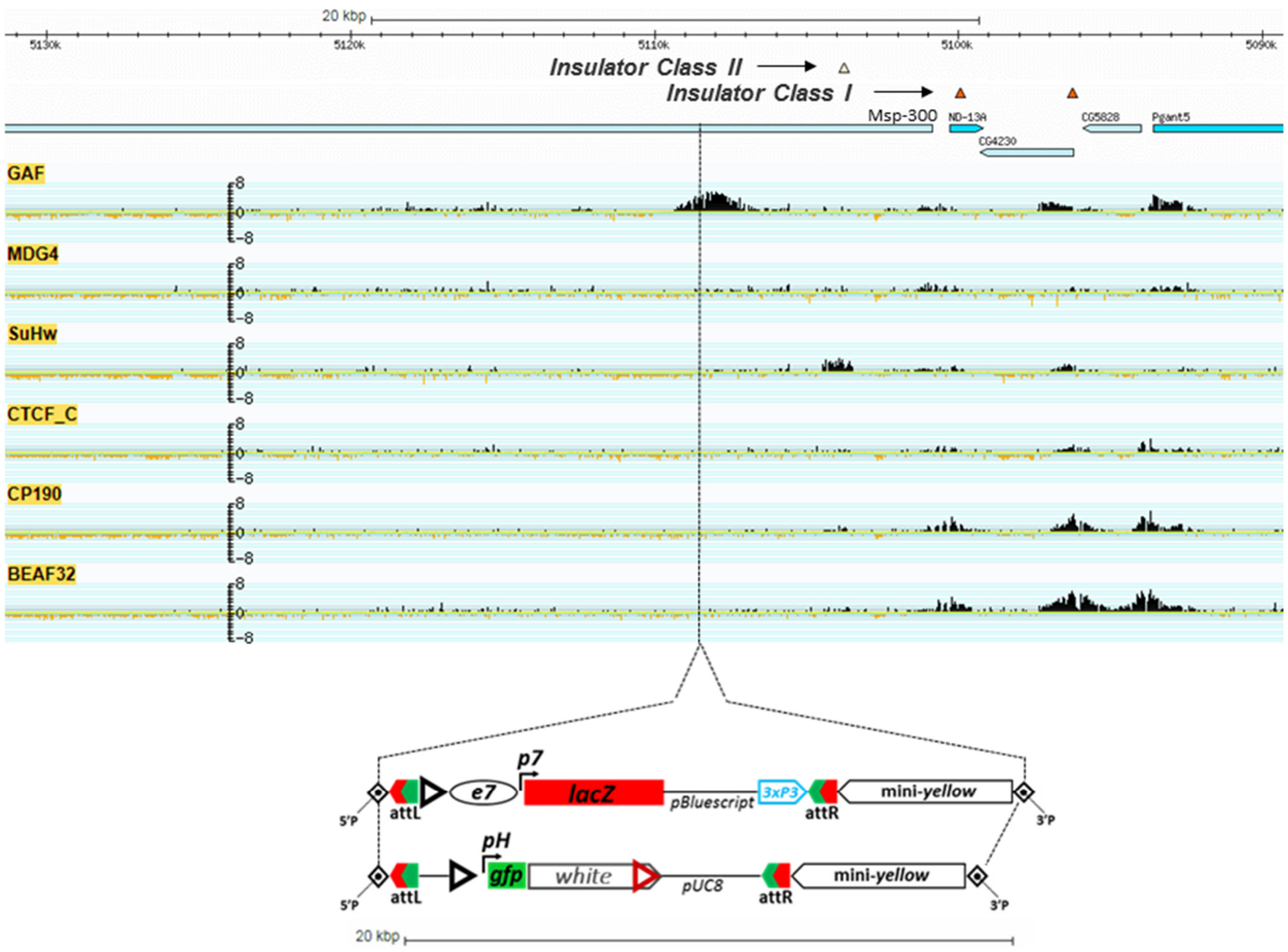

Figure S9 Genomic maps of transgene insertions used in **Figure S8**. The inserted transgenes are shown in the same scale as the genomic map. Note that only the GI-containing version of the two transgenes is shown. Our constructs are flanked by *attL* and *attR*, generated by *φC31*-integrase-mediated recombination to the different *attP* landing sites. mini-*yellow* and the two *Piggybac* (3'PBac, 5'PBac) or *P-element* (5'P, 3'P) ends come from the landing site. The remaining symbols are the same used in all other construct schematics in this work. Information is given on the chromatin occupancy of six insulator binding proteins (Celniker *et al.* 2009) and on the position of putative insulators (Negre *et al.* 2010) in the neighborhood of the insertion sites. For *VK37* and *attP40*, we have inverted the genomic map (sequence coordinates decreasing left to right) in order to depict the inserts in their correct orientation.

Figure S10

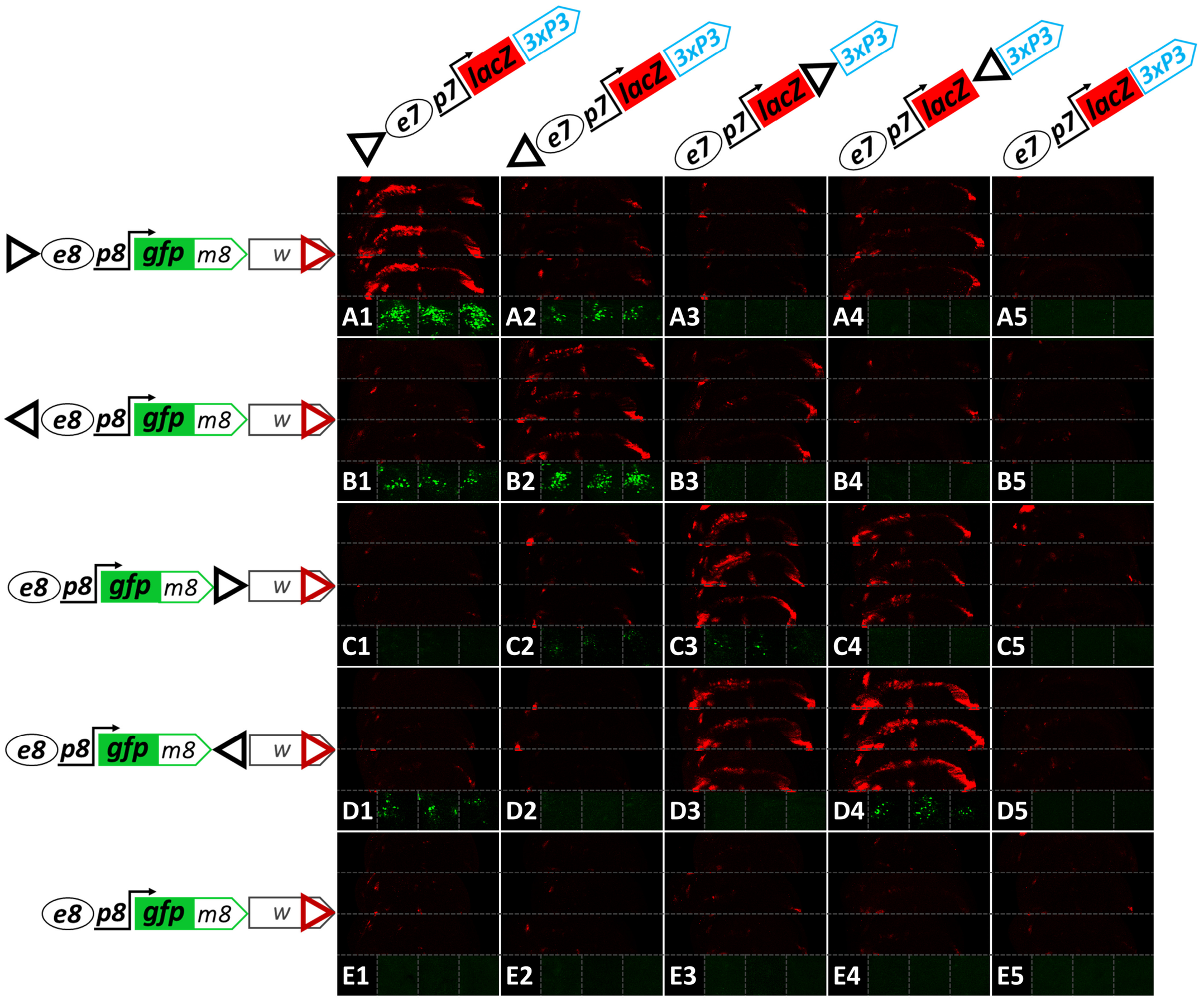

Figure S10 Less strict GI position and orientation requirements for interaction between *e7p7* and *e8p8*. (**A1**-**E5**) *e8p8-GFPm8* and *e7p7-lacZ* transgenes bearing a single GI are combined as shown in *attP40*. Each panel consists of six sub-panels containing confocal z-projections of the WM (only LacZ channel, in red) or the AMPs (only GFP channel, in green) from three different wing disks for each genotype. Both of these expressions result from transvection and are abrogated when one or both homologs lack a GI (row **E** and column **5**). Note, that unlike *e7p7→pH* transvection (**Figure 7 H**), *e8p8→e7p7* transvection (LacZ in the WM) is also mediated by the 3'GIs (**C3, C4, D3, D4**). The 3' GIs also mediate weak *e7p7→e8p8* transvection (GFP in AMPs), when congruently oriented (**C3, D4**). Note, also, that the absolute orientation of 5' GIs is less important for *e7p7→e8p8* transvection (compare GFP in **A1, A2, B1, B2**) than for *e7p7→pH* (**Figure 7 I, L**).

Figure S11

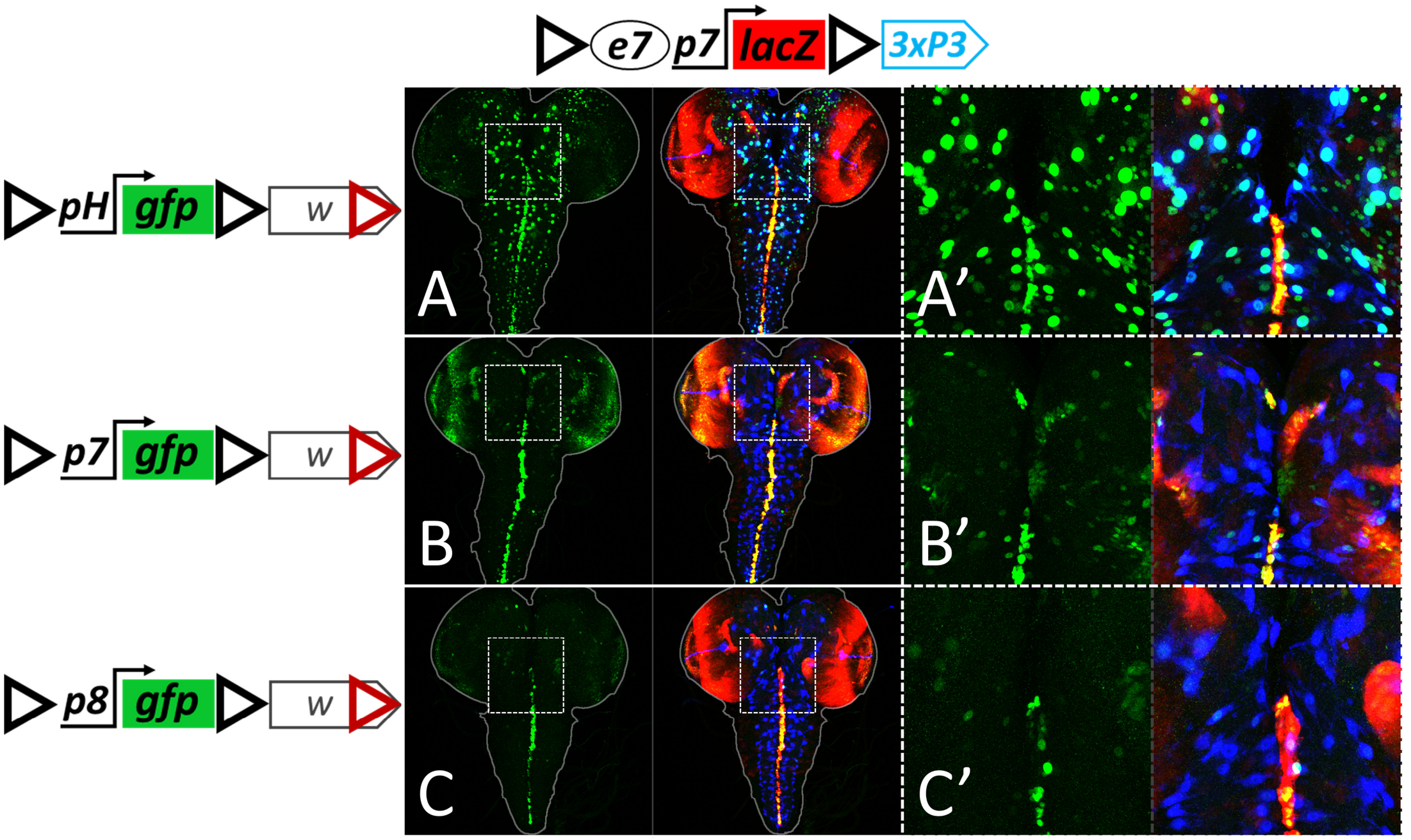

Figure S11 The *3xP3* enhancer has a stronger affinity for *pH* than for two other promoters. (**A**-**C**) Confocal z-projections of third instar CNSs showing GFP channel alone (green) and merged channels of GFP (green), LacZ (red) and DsRed (blue). (**A'**-**C'**) Enlarged regions of the central brains indicated by white rectangles in **A**-**C**. Out of the three enhancerless dual-GI^{FOR} *gfp* transgenes, each carrying a different promoter (**A** - *pH*, **B** - *p7*, **C** - *p8*), only the *pH*-driven reporter shows robust interaction with *3xP3* in the dual-GIs^{FOR} *e7p7-lacZ-3xP3* transgene in *attP40,* giving a dotty glial GFP pattern (**A, A'**). Notice weaker and sporadic GFP expression from *trans-3xP3* by *p7* (**B, B'**), even though *p7* is a stronger promoter than *pH*. In contrast, the "vertical" interaction of *e7* with the *trans* promoter (GFP in VNC midline and optic lobes) is stronger with *p7* (**B**) than with *p8* or *pH* (**A**, **C**).

Literature Cited

Celniker S. E., L. A. L. Dillon, M. B. Gerstein, K. C. Gunsalus, S. Henikoff, *et al.*, 2009 Unlocking the secrets of the genome. Nature 459: 927–930. https://doi.org/10.1038/459927a

Kim A., C. Terzian, P. Santamaria, A. Pelisson, N. Purd'homme, *et al.*, 1994 Retroviruses in invertebrates: the gypsy retrotransposon is apparently an infectious retrovirus of Drosophila melanogaster. Proc Natl Acad Sci U S A 91: 1285–1289.

Negre N., C. D. Brown, P. K. Shah, P. Kheradpour, C. A. Morrison, *et al.*, 2010 A comprehensive map of insulator elements for the Drosophila genome. PLoS Genet 6: e1000814. https://doi.org/10.1371/journal.pgen.1000814

Spana C., D. A. Harrison, and V. G. Corces, 1988 The Drosophila melanogaster suppressor of Hairy-wing protein binds to specific sequences of the gypsy retrotransposon. Genes Dev 2: 1414–1423.

Thurmond J., J. L. Goodman, V. B. Strelets, H. Attrill, L. S. Gramates, *et al.*, 2019 FlyBase 2.0: the next generation. Nucleic Acids Res. 47: D759–D765. https://doi.org/10.1093/nar/gky1003